Article:
Man, K, Mekhileri, NV, Lim, KS et al. (3 more authors) (2021) MI192 induced epigenetic reprogramming enhances the therapeutic efficacy of human bone marrows stromal cells for bone regeneration. Bone, 153. 116138. ISSN 8756-3282

https://doi.org/10.1016/j.bone.2021.116138

MI192 induced epigenetic reprogramming enhances the therapeutic efficacy of human bone marrows stromal cells for bone regeneration

Kenny Man[1, 2], Naveen Mekhileri[3], Khoon Lim[3], Lin-Hua Jiang[4], Tim Woodfield[3] and Xuebin B Yang[1*]

[1]Biomaterial and Tissue Engineering Group, School of Dentistry, University of Leeds, Leeds UK.
[2]School of Chemical Engineering, University of Birmingham, Birmingham, UK.
[3]CReaTE Group, Department of Orthopaedic Surgery, University of Otago, Christchurch, NZ.
[4]School of Biomedical Sciences, University of Leeds, Leeds, UK.

*Correspondence: x.b.yang@leeds.ac.uk

Biomaterials and Tissue Engineering Group
Department of Oral Biology
University of Leeds
Level 7, Wellcome Trust Brenner Building
St James's University Hospital
Leeds LS9 7TF, United Kingdom

Abstract

Human bone marrow stromal cells (hBMSCs) have been extensively utilised for bone tissue engineering applications. However, they are associated with limitations that hinder their clinical utility for bone regeneration. Cell fate can be modulated via altering their epigenetic functionality. Inhibiting histone deacetylase (HDAC) enzymes have been reported to promote osteogenic differentiation, with HDAC3 activity shown to be causatively associated with osteogenesis. Therefore, this study aimed to investigate the potential of using an HDAC2 & 3 selective inhibitor - MI192 to induce epigenetic reprogramming of hBMSCs and enhance its therapeutic efficacy for bone formation. Treatment with MI192 caused a time-dose dependant reduction in hBMSCs viability. MI192 was also found to substantially alter hBMSCs epigenetic function through reduced HDAC activity and increased histone acetylation. hBMSCs were pre-treated with MI192 (50 μM) for 48 hrs prior to osteogenic induction. MI192 pre-treatment significantly upregulated osteoblast-related gene/protein expression (Runx2, ALP, Col1a and OCN) and enhanced alkaline phosphatase specific activity (ALPSA) (1.43-fold) ($P \leq 0.001$). Moreover, MI192 substantially increased hBMSCs extracellular matrix calcium deposition (1.4-fold) ($P \leq 0.001$) and mineralisation when compared to the untreated control. In 3D microtissue culture, MI192 significantly promoted hBMSCs osteoblast-related gene expression and ALPSA (> 2.41-fold) ($P \leq 0.001$). Importantly, MI192 substantially enhanced extracellular matrix deposition (ALP, Col1a, OCN) and mineralisation (1.67-fold) ($P \leq 0.001$) within the bioassembled-microtissue (BMT) construct. Following 8-week intraperitoneal implantation within nude mice, MI192 treated hBMSCs exhibited enhanced extracellular matrix deposition and mineralisation (2.39-fold) ($P \leq 0.001$) within the BMT when compared to the untreated BMT construct. Taken together, these results demonstrate that MI192 effectively altered hBMSCs epigenetic functionality and is capable of promoting hBMSCs osteogenic differentiation *in vitro* and *in vivo*, indicating the potential of using epigenetic reprogramming to enhance the therapeutic efficacy of hBMSCs for bone augmentation strategies.

Keywords: HDAC inhibitor, histone deacetylase, osteogenic differentiation, MI192, bone marrow stromal cells, bone tissue engineering, epigenetics, additive manufacturing

Introduction

There is a tremendous need for clinically relevant bone tissue for the treatment of critical-sized bone defects caused by numerous situations such as traumatic injury and age-associated disorders, including osteoporosis [1]. This clinical need is expected to increase in the future due to the growing ageing population. Current therapies such as autografts are associated with drawbacks such as their limited availability and donor site morbidity [2, 3]. As such, there is great precedence for new approaches to regenerate damaged/lost bone. Hence, extensive research has been conducted within the tissue engineering field to meet the rising demand for bone tissue. For cell-based therapies, controlling mesenchymal stromal cells (MSCs) osteogenic differentiation is a key factor for the development of functional engineered bone [4]. Although extensively utilised, there has been limited clinical success with the use of MSCs for bone repair due to their low procurement yield, inherent heterogeneity, and the need for extensive *in vitro* expansion [5]. While methods such as gene therapy have been used to enhance MSCs clinical efficacy, this approach is cost-intensive and poses a risk of tumourigenesis [6].

It has become increasingly apparent that epigenetics plays a significant role in regulating cell fate. Specifically, researchers have demonstrated that post-translational modifications such as the process of acetylation result in alterations in the chromatin structure, regulated by two histone-modifying enzymes [7]. Histone acetyltransferase (HAT) is responsible for acetylation, resulting in the opening of the chromatin structure and enhanced transcriptional activity, while deacetylation activity from histone deacetylase (HDAC) causes chromatin condensation leading to transcriptional repression [7-9]. Several studies have induced hyperacetylation through the use of HDAC inhibitors (HDACis) which has been reported to enhance MSCs osteogenic capacity [10-12]. Although epigenetic approaches have shown promise, non-selective panHDACis have been primarily utilised, which inhibits a broad range of HDAC isoforms. This may result in off-target effects such as inducing apoptosis and inhibiting the cells' differentiation efficacy [13]. Hence, there is great precedence to shift towards a selective approach. Studies have reported that HDAC3 is causatively associated with osteogenic differentiation due to its role in repressing the activity of the osteogenic transcription factor, Runx2 [14, 15]. MI192, an HDAC2 & 3 selective inhibitor, has demonstrated its efficacy in the fields of rheumatoid arthritis, leukaemia and neuroregeneration research [16-18]. The increased selectivity in which MI192 targets HDAC3 may provide a novel approach to enhance MSCs efficacy for bone formation. Recently, it has been reported that MI192 significantly promoted the mineralisation capacity of human dental pulp stromal cells (hDPSCs) in 2D *in vitro* culture[19], indicating the efficacy of this engineering approach for bone augmentation strategies.

While HDACis efficacy in promoting MSCs differentiation has been reported, these investigations have primarily been conducted in 2D *in vitro* culture. 2D culture limits the cell-cell and cell-extracellular matrix interactions, which do not replicate *in-situ* conditions mechanically or biologically [20, 21]. Several studies have demonstrated the increased osteoinduction of MSCs when cultured in 3D compared to conventional 2D culture [22, 23]. Moreover, it has been reported that cells exhibit altered receptiveness to bioactive signals when cultured in 3D [21]. Hence, there is a tremendous need to investigate the osteoinductive efficacy of selective HDACis in more physiological 3D culture environments. Studies have shown that spheroid culture (microtissues) enhances MSCs mineralisation [24, 25], due to facilitating cell-cell/cell-extracellular matrix interactions [22]. Although the use of microtissues has shown promise for bone repair [22], their inherent lack of mechanical strength limits

their clinical application for load-bearing tissues. Advances in additive manufacturing and biofabrication have allowed for increasing control for engineering functional tissue [26]. In particular, modular assembly approaches where cellular components are combined with structural scaffolds has created functional constructs that possess huge potential for bone tissue engineering. An example of this modular assembly strategy is the bioassembled-microtissue (BMT) construct [27]. This model consists of assembling pre-cultured microtissues with a 3D printed porous scaffold, therefore harnessing the advantages of spheroid culture for bone formation, while the 3D printed scaffold provides both spatial control of microtissues and structural support for load-bearing defects [27, 28]. Hence, the BMT model offers a platform to assess the efficacy of MI192 in stimulating bone-like tissue formation in a more physiologically relevant model.

Therefore, this study aimed to examine the effects of MI192 epigenetic reprogramming on the behaviour and osteogenic differentiation of human bone marrow stromal cells (hBMSCs) in 2D and 3D *in vitro* and *in vivo*. The effects of MI192 on hBMSCs viability and epigenetic functionality was evaluated. MI192 optimum treatment regimen (50 µM for 48 hours) was determined to effectively promote hBMSCs osteogenic differentiation and mineralisation capacity. Within the BMT construct, the efficacy of MI192 treatment on stimulating hBMSCs bone formation was evaluated *in vitro* and *in vivo.*

Materials and Methods

Cell culture and reagents

hBMSCs were purchased from Lonza (Lonza, UK) (n = 2; 33 and 41 years of age), and the trilineage potential verified (Supplementary figure 1). Cells were maintained in basal media, containing alpha modified minimum essential medium (α-MEM, Lonza, UK) supplemented with 10% fetal calf serum (FCS, Sigma-Aldrich, UK) and 100 units/ml penicillin with 100 µg/ml streptomycin (Sigma-Aldrich, UK), at 37°C in 5% CO_2 until 80% confluent. The cells at passage 4 were used for this study. 100 mM MI192 (Sigma-Aldrich, UK) stock solution was prepared fresh in sterile-filtered dimethyl sulfoxide (DMSO, Sigma-Aldrich, UK) and this stock was further added to the culture medium to make the desired concentration. The DMSO percentage in the 50 µM MI192 working solution was 0.05%, a percentage reported to not induced cytotoxicity [29, 30].

Cell viability and morphology assessment

Cells (1 x 10^4 cells/well) were seeded within a 96-well plate and incubated in basal medium for 24 hours. The medium was replaced with fresh basal medium supplemented with/without MI192 (1, 10, 20, 50 µM) and incubated for 24, 48 and 72 hours. AlamarBlue reagent (Thermo Scientific, UK) was added to each well and incubated for 4 hours at 37°C. Fluorescence readings were acquired using a Varioskan Flash Multimode Microplate Reader (Thermo Scientific, UK) at 540/590 nm wavelength. For morphological assessment, cells were seeded (1 x 10^5 cells/well) in a 24-well plate and incubated for 24 hours, after which the same treatment regime was utilised. Cell morphology was evaluated using a Zeiss Axio Vert.A1 (Carl Zeiss, Oberkochen, Germany).

DNA quantification

DNA quantification was determined by Quant-iT PicoGreen DNA assay (Invitrogen, Life Technologies, UK). Briefly, 10 µl of cell lysate (in 0.1% Triton^{TM} X-100) was added to 90 µl of TE (10 mM Tris-HCl, 1 mM EDTA) buffer into a 96-well plate (Corning, UK). 100 µl of PicoGreen reagent was added to all samples and incubated for 5 minutes. The fluorescence was then measured in a Varioskan Flash Multimode Microplate Reader at 480/520 nm wavelength.

HDAC activity and H3K9 histone acetylation

Cells were cultured in 96-well plates (1 x 10^4 cells/well) in basal medium for 24 hours. The medium was replaced with fresh basal medium supplemented with/without MI192 (1, 5, 10, 20, 50 µM). At 24 and 48 hours, the medium was replaced with 100 µl of reaction mix (*in situ* HDAC activity fluorometric assay kit: Biovision, UK) and incubated for 3 hours at 37^{o}C. 100 µl of lysine developer was added then incubated for a further 30 minutes at 37^{o}C. The fluorescence was measured in a Varioskan Flash Multimode Microplate Reader (Thermo Scientific, UK) at 368/442 nm wavelength. HDAC activity was normalised with total DNA content.

EpiQuikTM *In Situ* Histone H3-K9 Acetylation Assay Kit (Epigentek, USA) was used for detecting H3K9 acetylation according to the manufacturer's protocol. The absorbance was read in a Varioskan Flash Multimode Microplate Reader (Thermo Scientific, UK) at 450 nm. Histone acetylation was normalised with the total DNA content.

Osteogenic induction culture

Untreated or MI192 pre-treated cells were cultured in osteogenic medium, consisting of basal medium supplemented with 50 µM L-ascorbic acid 2-phosphate sesquimagnesium salt hydrate, 10 mM β-glycerol phosphate and 100 nM dexamethasone (Sigma-Aldrich, UK). The medium was changed every 3 days.

Alkaline phosphatase specific activity (ALPSA) quantification assay

ALPSA was determined using the 4-nitrophenyl colourimetric phosphate liquid assay (pNPP, Sigma-Aldrich, UK). 90 µl of pNPP was added to 10 µl of cell lysate and incubated for 60 minutes at 37°C. The absorbance at 405 nm was read on a Varioskan Flash Multimode Microplate Reader (Thermo Scientific, UK). ALP activity was normalised with total DNA content.

Quantitative RT-qPCR analysis

RNA was extracted using the RNase mini kit (Qiagen, UK), and then 200 ng of RNA was transcribed to cDNA using the high capacity RNA to cDNA Kit (Applied Biosystems, UK) following the manufacturer's instructions. Thereafter, the cDNA was amplified using TaqMan primers (supplementary table 1) in a 20 µl reaction within a 96-well PCR plate (Starlab, UK). Amplification occurred within a LightCycler 480 real-time qPCR system (Roche, UK). For each sample, the cycle threshold (Ct) value was acquired, and the comparative Ct method ($2^{-\Delta\Delta Ct}$) was utilised to quantify the gene expression levels relative to the housekeeping gene GAPDH.

In-Cell Western (ICW) assay

Following fixation in 10% (v/v) neutral buffered formalin (NBF, Cellpath, UK), cells were permeabilised with 0.1% Triton™ X-100. The samples were incubated overnight at 4°C with primary antibodies (supplementary table 2) against osteocalcin (1:400), Runx2 (1:500), alkaline phosphatase (1:300) and collagen type I (1:200) (Abcam, UK) in Odyssey® buffer. Samples were incubated with the IRDye 800CW secondary antibody (1:800) with the CellTag™ 700 stains (1:500; Li-Cor Biosciences, UK) in the Odyssey blocking buffer (Li-Cor Biosciences, UK) for 1 hour, prior to scanning on the Odyssey SA Imaging System (Li-Cor Biosciences, UK) using both 700 and 800 nm detection channels. Quantitative analysis was performed using the Image Studio (Li-Cor Biosciences: version 5).

Scaffold fabrication

Bio-degradable poly (ethylene glycol)-terephthalate-poly (butylene terephthalate) (PEGT/PBT) block copolymers were defined by a PEG molecular weight of 300 g/mol and a PEGT:PBT weight per cent (wt%) ratio of 55:45 as previously described [27]. Briefly, scaffolds were fabricated in a layer by layer process using 3D BioPlotter (EnvisionTEC, Germany) with a 1 mm fibre spacing. Fibres were oriented in a 0 - 90° pattern in a bi-layered fashion. Scaffolds with dimensions of approximately 3.3 × 2.1 × 2.1 mm^3 were sterilised in 70% ethanol overnight and washed thoroughly with PBS prior to use.

Bioassembled-microtissue culture

250 µl hBMSCs suspension (untreated or 50 µM MI192 treated for 48 hours) (2.5×10^5 cells) was added into a V-bottom 96-well plate (Greiner Bio-One, UK) and centrifuged at 300 *g* for 4 minutes. The osteogenic medium was changed every two days for up to one week to allow microtissue formation. Then, the microtissues were transferred into the pores of the 3D printed scaffolds (1 pellet per pore) to form the BMT construct [27]. A total of 8 pellets were incorporated into the scaffold in a bi-layered configuration (4 microtissues per layer). Constructs were cultured in osteogenic medium for 6 weeks.

Histological and immunohistochemical analysis

Following fixation in 10% neutral buffered formalin (NBF) (Cellpath, UK), samples were embedded in paraffin wax and sectioned (4 µm) using a microtome (Leica, UK). Sections were stained with Haematoxylin and Eosin (H&E) (Sigma-Aldrich, UK), Picrosirius red (Abcam, UK)/Alcian blue (Sigma-Aldrich, UK), using standard histological methods. Calcium deposits were identified with Alizarin red (2% pH 4.3) for 15 mins. For semi-quantification, Alizarin red-stained samples were de-stained with 10% cetylpyridinium chloride (Sigma-Aldrich, UK) for 1 hour and then absorbances were read at 550 nm using the Varioskan Flash Multimode Microplate Reader. Mineralisation was assessed using the Von Kossa Staining Kit (Atom Scientific, UK) following the manufacturer's instructions. The mean mineral nodule percentage coverage was quantified using ImageJ software.

Extracellular matrix deposition was assessed using the EnVision™ Detection Systems Peroxidase/DAB, Rabbit/Mouse (Dako, UK). Briefly, sections were placed in a PBS bath before incubation with 'Dual Endogenous Enzyme Block' from the EnVision™ kit for 10 mins. Sections were washed in PBS for 5 mins prior to blocking by 20% Normal goat serum (Dako, UK) in PBS for 30 mins. Then, the primary antibodies (supplementary table 2) were added to samples at the desired concentration in 1% BSA (Sigma-Aldrich, UK) in PBS and incubated overnight at 4 °C. The next day, sections were washed in PBS

for 10 mins, before the addition of the secondary antibody HRP goat anti-rabbit to sections for 30 mins. After PBS wash for 5 mins, the Dako DAB developing solution was added to sections for 10 mins before immersion in Harris Haematoxylin for 20 seconds, which was cleared in a running water bath. Slides were then dehydrated, mounted and visualise under the microscope (Olympus BX50).

In vivo implantation of BMTs

All procedures for the animal studies were conducted under the approval of the University of Leeds Ethics Committee and under the UK Home Office project license (PPL: 70/8549). Untreated and MI192 treated BMTs were fabricated as described above. The constructs (n=5) were sealed within diffusion chambers (Sigma-Aldrich, UK), which was then implanted within the intraperitoneal cavity of immunocompromised CD1 nude mice (30 g, 8-week old male). After 8 weeks, the chambers were retrieved, and samples were fixed in 10% NBF prior to histological and immunohistochemical analysis.

Data analysis

For all data presented, experiments were repeated at least 3 times. All statistical analysis was undertaken using ANOVA multiple comparisons test with Tukey modification with IBM SPSS software (IBM Analytics, version 21). P values equal to or lower than 0.05 was considered significant. *$P \leq 0.05$, **$P \leq 0.01$ and ***$P \leq 0.001$.

Results

MI192 altered hBMSCs epigenetic functionality in 2D *in vitro*

Following 24 hours of culture, cells in the basal medium exhibited a fibroblast-like morphology (Fig 1A). Treatment with low concentrations of MI192 (≤ 10 μM) exhibited a similar fibroblast-like morphology as the control, while treatment with higher concentrations (20 and 50 μM) resulted in a dose-dependent reduction in cell density whilst also exhibiting a condensed morphology. At 48 and 72 hours, a more apparent dose-dependent reduction in cell density was observed with an increasing quantity of floating cells in the high MI192 concentration groups. The AlamarBlue assay showed that MI192 caused a time and dose-dependent reduction in hBMSCs metabolic activity when compared to that of the untreated control (Fig 1B). MI192 concentrations of ≥ 20 μM, ≥ 10 μM and ≥ 1 μM significantly reduced hBMSCs viability at 24, 48 and 72 hours ($P \leq 0.01, 0.001, 0.001$, respectively).

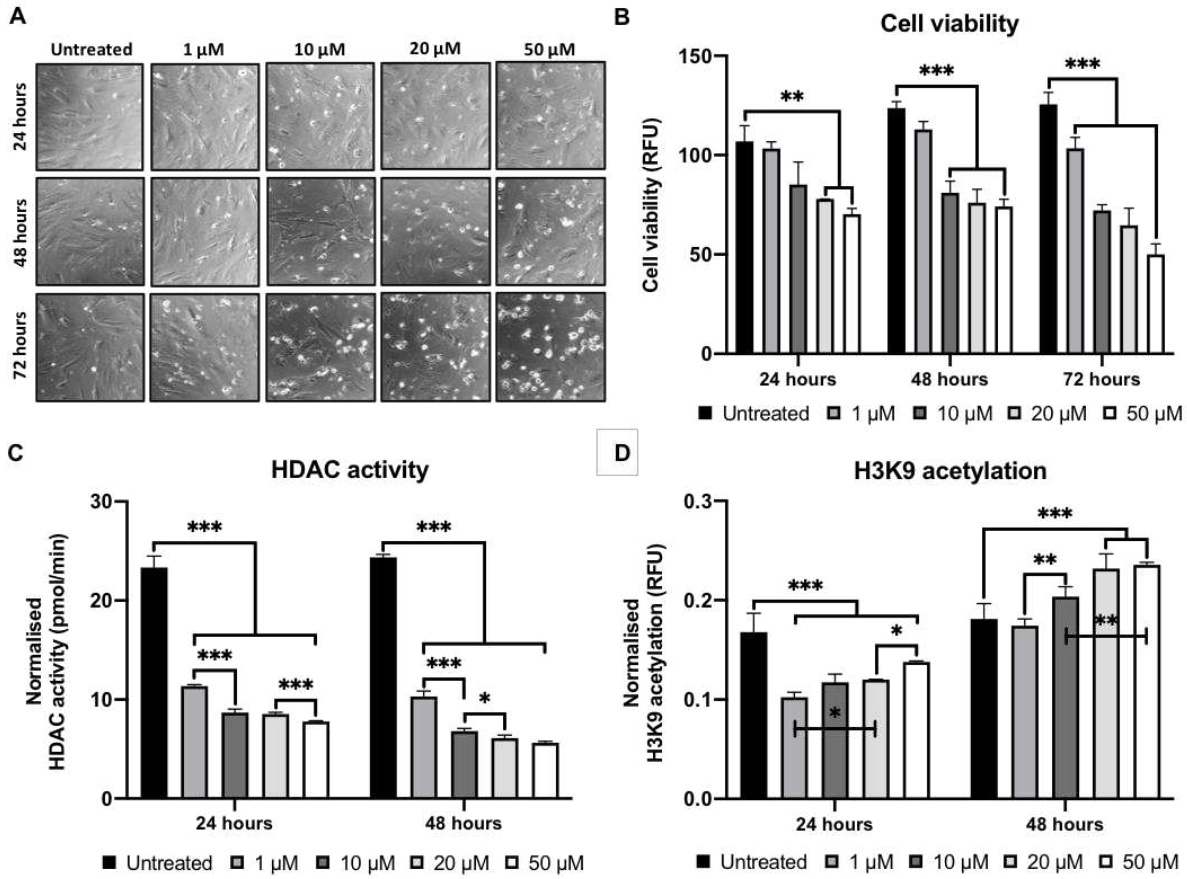

Figure 1 - The effects of MI192 on hBMSC viability and epigenetic functionality. MI192 caused a time-dose dependant effect on hBMSCs A) morphology (magnification x 100), B) metabolic activity, C) HDAC activity and D) H3K9 histone acetylation levels. Data are represented as mean ± SD (n = 3). *P ≤ 0.05, **P ≤ 0.01 and ***P ≤ 0.001.

HDAC activity assay showed that MI192 treatment (1 - 50 µM) led to a significant time- and dose-dependent reduction in HDAC activity compared to the untreated control (Fig 1C) (P ≤ 0.001). At 24 hours, there was a significant reduction in HDAC activity of the 10 µM vs 1 µM treated group, and 50 µM vs 20 µM group (P ≤ 0.001). Similarly, there were significant reductions in HDAC activity in 10 µM vs 1 µM group (P ≤ 0.001), and 20 µM vs 10 µM group (P ≤ 0.05) at 48 hours.

All test groups treated with MI192 for 24 hours caused a significant reduction in the histone acetylation levels when compared to the untreated cells (P ≤ 0.001), with a dose-dependent increase in acetylation observed within the MI192 treated groups. The 20 µM and 50 µM MI192 treated cells exhibited a significant increase in acetylation levels compared to the 1 µM and 20 µM treated groups respectively (P ≤ 0.05). At 48 hours, there was a dose-dependent increase in histone acetylation, with 20 and 50 µM groups exhibiting a significant increase in acetylation levels compared to the untreated cells (P ≤ 0.001). Interestingly, there was a significant enhancement in acetylation within the 20 µM vs 10 µM group (P ≤ 0.05), and 10 µM vs 1 µM group (P ≤ 0.01) (Fig 1D).

MI192 promoted hBMSCs osteogenic differentiation and mineralisation in 2D *in vitro*

The influence of MI192 pre-treatment for 24 or 48 hours on hBMSCs osteogenic differentiation after 14 days osteogenic culture was evaluated by assessing ALPSA (Fig 2). Cells pre-treated with MI192 for 24 hours exhibited significantly reduced ALPSA when compared to untreated hBMSCs cultured in osteogenic medium (≥ 1.38-fold) ($P \leq 0.05$). Following pre-treatment with MI192 for 48 hours, ALPSA results showed that 50 µM MI192 significantly enhanced hBMSCs ALPSA (>1.43-fold) when compared with other MI192 doses and the untreated control following 14 days osteoinduction ($P \leq 0.001$). Thus, 50 µM MI192 pre-treatment for 48 hours was used for subsequent experiments.

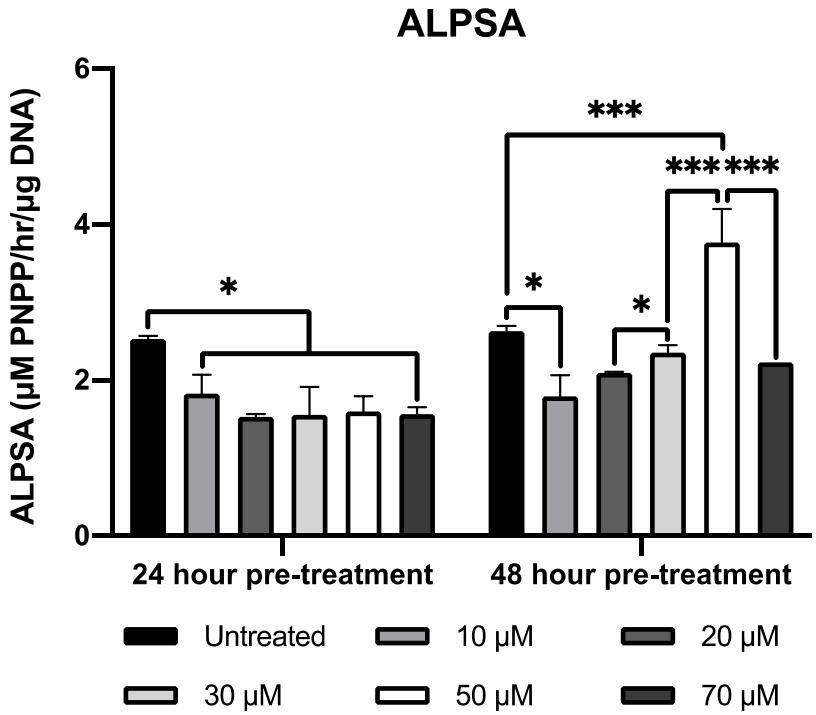

Figure 2 - Effect of MI192 pre-treatment on hBMSCs ALPSA. Cells were pre-treated with/without MI192 for 24 or 48 hours prior to culture in osteogenic medium for 14 days. Data are represented as mean ± SD (n=3). *$P \leq 0.05$ and ***$P \leq 0.001$.

After 50 µM MI192 pre-treatment and 3 days of osteogenic culture, RT-qPCR (Fig 3A) confirmed that the mRNA levels of the early osteogenic markers (*RUNX2* and *ALP*) were significantly upregulated in the MI192 pre-treated cells ($P \leq 0.05$), while the mRNA levels of later markers (*COL1A* and *OCN*) were slightly down-regulated compared to untreated cells, however not significantly ($P > 0.05$) (Fig 3A). On day 7, the mRNA expression of all osteoblast-related genes was significantly upregulated in MI192 pre-treated cells compared to that in the untreated control ($P \leq 0.05$). On day 14, a similar significant increase in gene expression was observed in the MI192 pre-treated cells ($P \leq 0.05$ - 0.01). On day 21, the mRNA expression remained upregulated in the MI192 pre-treated cells, with the expression of *RUNX2* significantly increased compared to the untreated control ($P \leq 0.01$).

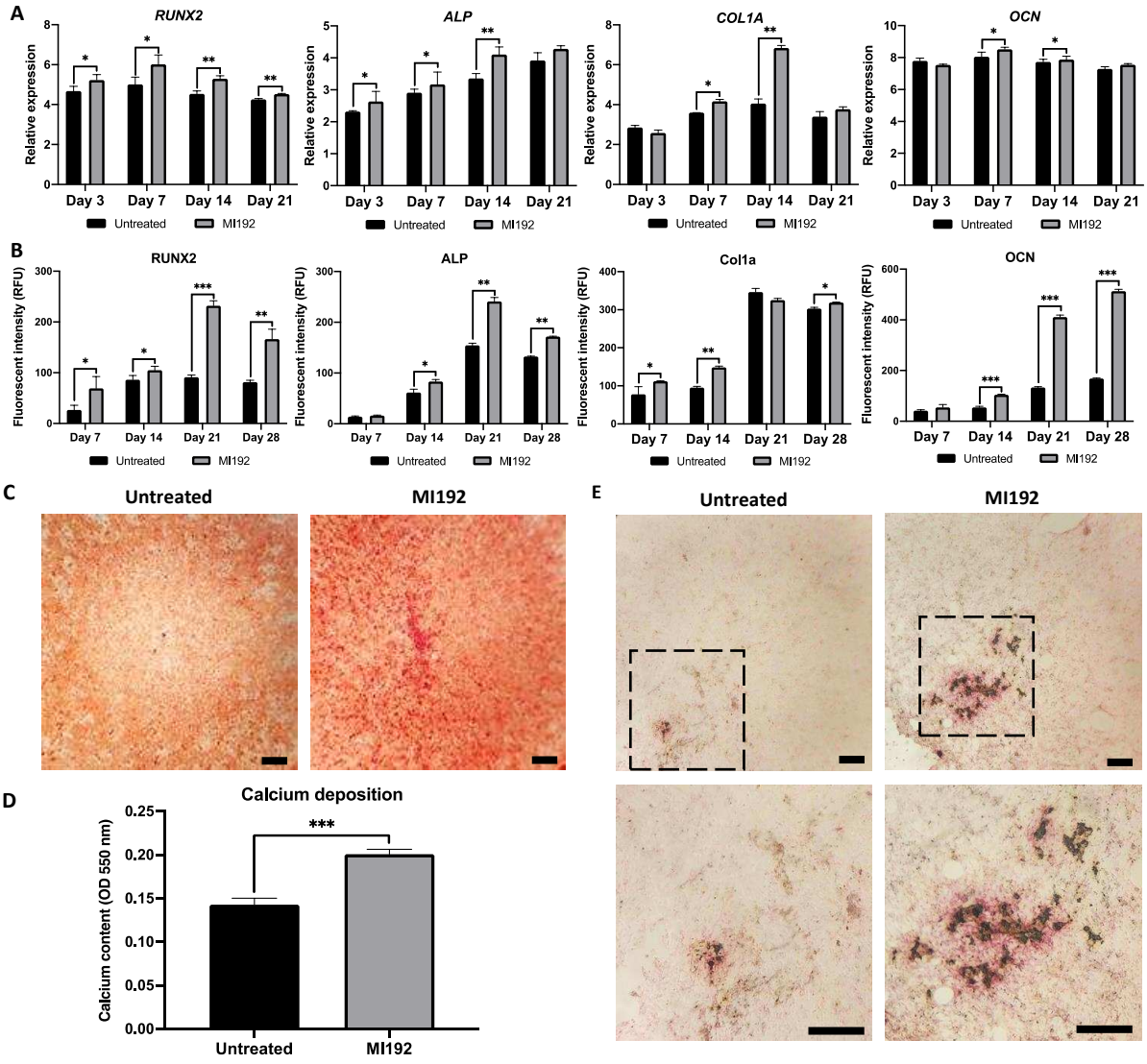

Figure 3 - The effects of MI192 on hBMSCs osteogenic differentiation and mineralisation. A) mRNA expression levels of *RUNX2, ALP, COL1A* and *OCN* were measured in untreated/MI192 pre-treated (50 µM for 48 hours) hBMSCs during osteoinductive culture. B) Protein expression levels of RUNX2, ALP, Col1a and OCN in untreated/MI192 pre-treated (50 µM for 48 hours) hBMSCs analysed by ICW. C) Alizarin Red staining for calcium deposition (x100), D) Semi-quantification of Alizarin Red staining, and E) Von Kossa staining of hBMSCs untreated/MI192 pre-treated (50 µM for 48 hours) hBMSCs after 28 days of osteoinductive culture. Black squares highlight the magnified area in the panel below. Scale bars = 100 µm. Data are represented as mean ± SD (n=3). *P ≤ 0.05, **P ≤ 0.01 and ***P ≤ 0.001.

ICW was used to examine the effects of 50 µM MI192 pre-treatment on the intracellular expression of osteoblast-related proteins (Runx2, ALP, Col1a and OCN) (Fig 3B). On day 7, MI192 pre-treatment significant enhanced hBMSCs protein expression levels for Runx2 and Col1a compared to that of the control group (P ≤ 0.05 - 0.01). However, there was no significant difference for ALP, and OCN protein expression between the MI192 treated and untreated cells (P > 0.05) (Fig 3B). On day 14, all markers assessed were significantly increased in the MI192 pre-treated cells compared to that of the control group (P ≤ 0.05 - 0.001). A similar significant upregulation was observed at day 21 (P ≤ 0.01 - 0.001), with Col1a expression levels similar to the untreated control (P > 0.05). On day 28, the expression of

all osteoblast-related proteins were significantly enhanced in the MI192 treated cells compared to the untreated control ($P \leq 0.05$ - 0.001).

Alizarin red staining showed that the MI192 treated group substantially enhanced hBMSCs extracellular matrix calcium deposition compared to the untreated control (Fig 3C). The semi-quantitative analysis confirmed the MI192 pre-treated cells exhibited significantly enhanced calcium deposition (1.4-fold) compared to the untreated group ($P \leq 0.001$) (Fig 3D). Von Kossa staining indicated that there was a substantial increase in mineral nodule formation (black staining) in the MI192 pre-treated group compared to the untreated control (Fig 3E). Additionally, enhanced Van Gieson's staining for collagen deposition (pink staining) was observed in the MI192 pre-treated group, particularly in close proximity to the mineral nodules.

MI192 enhanced hBMSCs osteogenic differentiation and mineralisation in 3D BMT *in vitro*

Following pre-treatment with/without 50 µM MI192 for 48 hours, hBMSCs were cultured as microtissues in osteogenic conditions for up to 21 days, and the mRNA levels of osteoblast-related genes were assessed (Fig 4A). On day 7, the expression of *Col1α* and *OCN* were significantly upregulated in the MI192 pre-treated cells when compared to that in the untreated group ($P \leq 0.05$ - 0.01). On day 14, the expression of *ALP* was significantly enhanced in the MI192 pre-treated group ($P \leq 0.01$). The mRNA expression levels of *ALP* were significantly increased in the MI192 pre-treated cells when compared to that in the untreated group at day 21 ($P \leq 0.05$), while *OCN* was significantly down-regulated in the MI192 pre-treated group ($P \leq 0.05$). Following 2 weeks in osteogenic conditions, MI192 pre-treatment significantly enhanced hBMSCs ALPSA when compared to that of the untreated BMT construct (> 2.41-fold) ($P \leq 0.001$) (Fig 4B).

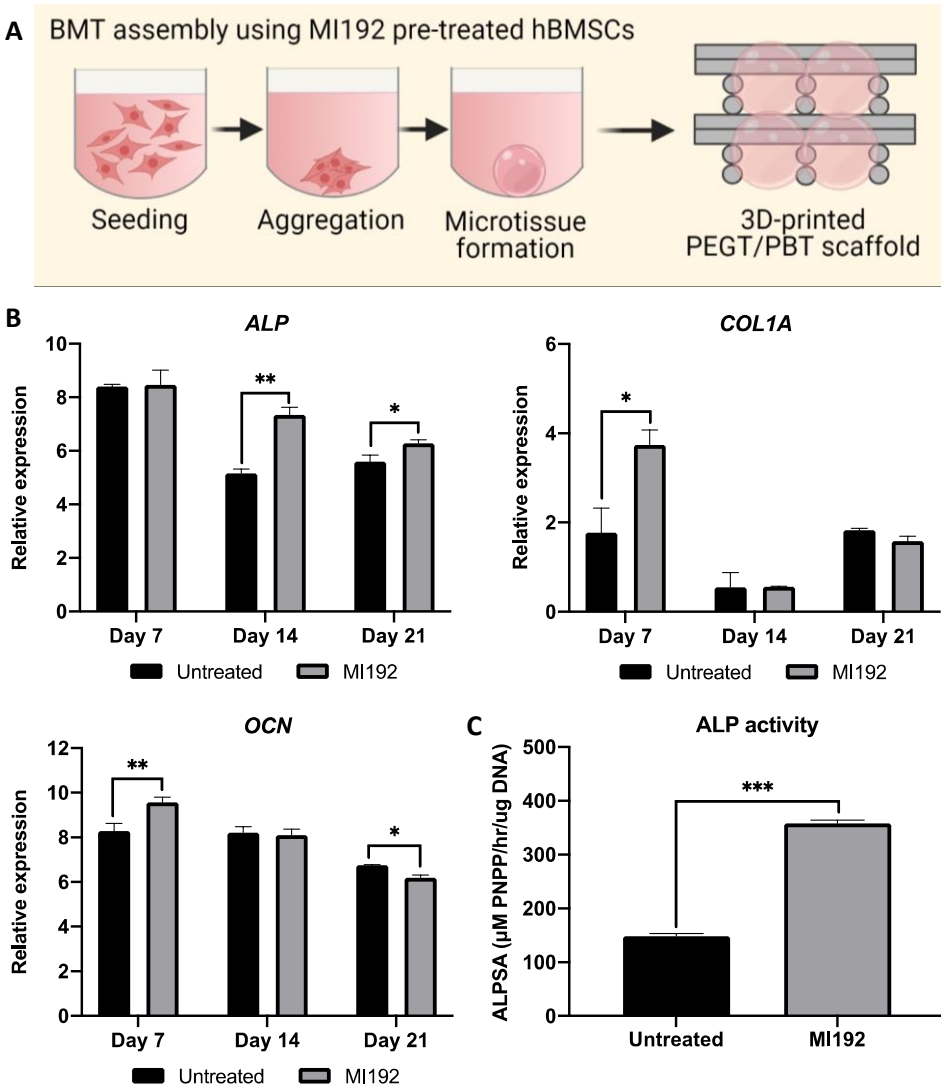

Figure 4 - The effects of MI192 on hBMSCs osteogenic differentiation within the 3D BMT construct *in vitro*. A) Schematic diagram represents the procedure of microtissues formation and the creation of the BMT construct (Created with BioRender.com). B) mRNA expression levels of *ALP, COL1A* and *OCN* were measured in untreated/MI192 pre-treated hBMSCs microtissues during osteoinductive culture. C) ALPSA of hBMSCs microtissues pre-treated with/without MI192, followed by 14 days in osteogenic conditions. Data are represented as mean ± SD (n=3). *P ≤ 0.05, **P ≤ 0.01 and ***P ≤ 0.001.

Histological analysis confirmed that the incorporated microtissues fused within the 3D printed scaffold after 6 weeks *in vitro* culture in osteogenic conditions (Fig 5A). The MI192 treated constructs exhibited enhanced uniformity in tissue formation when compared to the distribution observed within the untreated BMT. Moreover, the MI192 pre-treated group exhibited strong picrosirius red staining for collagen deposition throughout the construct. However, collagen staining in the untreated BMT was observed in an aberrant manner (Fig 5B). Additionally, GAGs deposition highlighted by alcian blue staining was substantially increased in the untreated group compared to the MI192 construct (Fig 5B). Von Kossa staining showed that both groups exhibited positive staining for functional mineral nodules (black staining). However, the mineralisation within the MI192 pre-treated group was distributed more homogenously throughout the construct when compared to the untreated control (Fig 5C). Semi-quantitative analysis indicated a significant increase in mineral nodule coverage in the MI192 pre-treated BMT constructs (1.67-fold) compared to the untreated control (Fig 5D) (P ≤ 0.001).

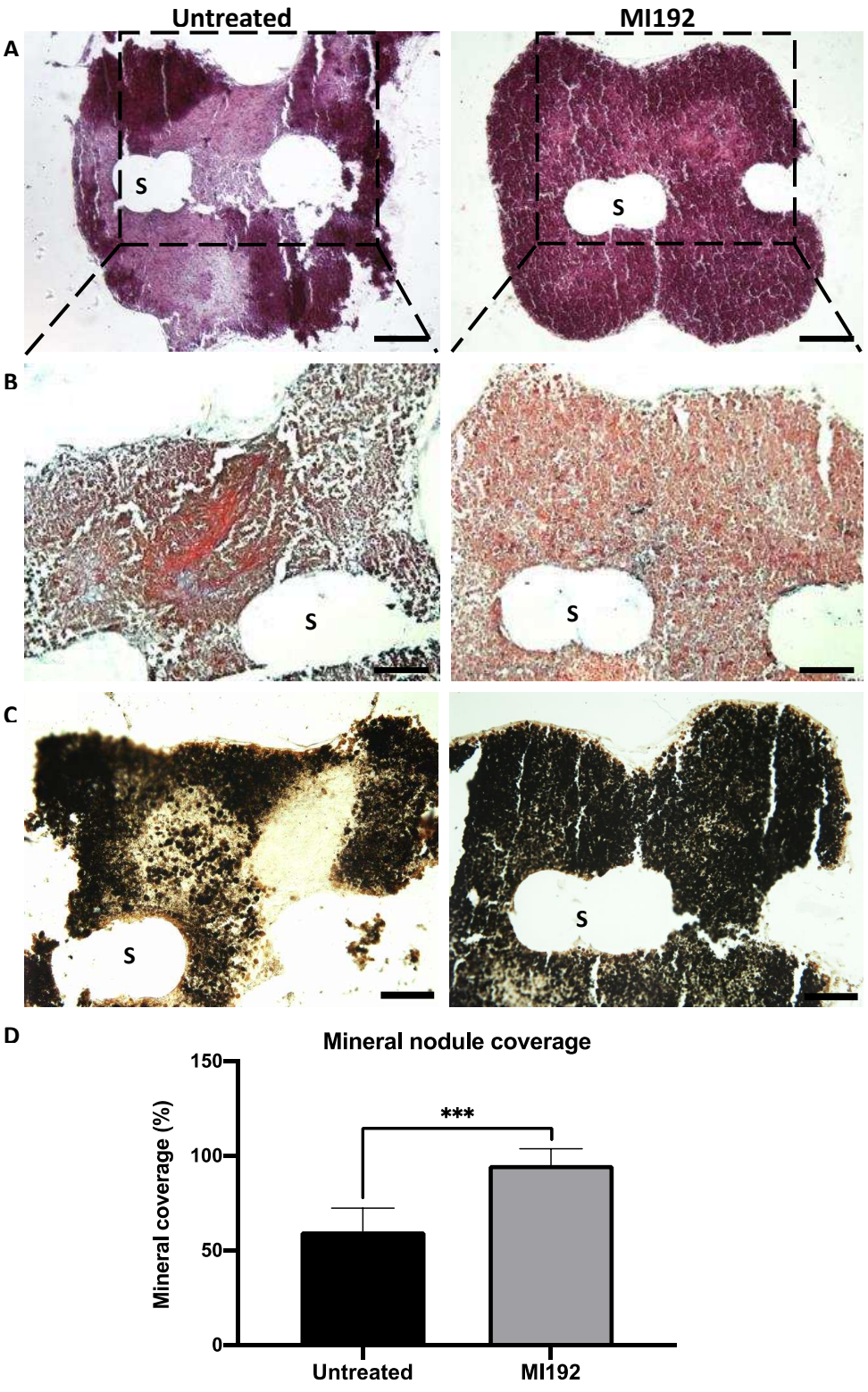

Figure 5 - MI192 promote hBMSCs *de novo* tissue formation in 3D BMT constructs after 6 weeks *in vitro* culture. A) H&E staining showing tissue formation within the BMT, B) Picrosirius red/alcian blue staining identifying collagen/GAG depositions within the construct, C) Mineral nodule formation highlighted by Von Kossa staining, D) Percentage mineral nodule coverage on BMT samples. Scale bars = 200 (A) and 100 µm (B, C), respectively. Data are represented as mean ± SD (n=3). ***P ≤ 0.001. 'S' denotes the spaces of '3D printed PEGT/PBT scaffolds', which were removed during histological processing.

Immunohistochemical analysis showed that both untreated and MI192 pre-treated BMT constructs exhibited positive staining for the osteoblast-related markers (ALP, Col1a and OCN), with enhanced protein deposition situated at the outer regions of individual microtissues and the periphery of the construct (Fig 6). The MI192 pre-treated BMTs displayed substantially increased deposition of ALP, Col1A and OCN when compared to the untreated construct. Moreover, protein expression was distributed more uniformly throughout the MI192 construct when compared to the untreated BMT.

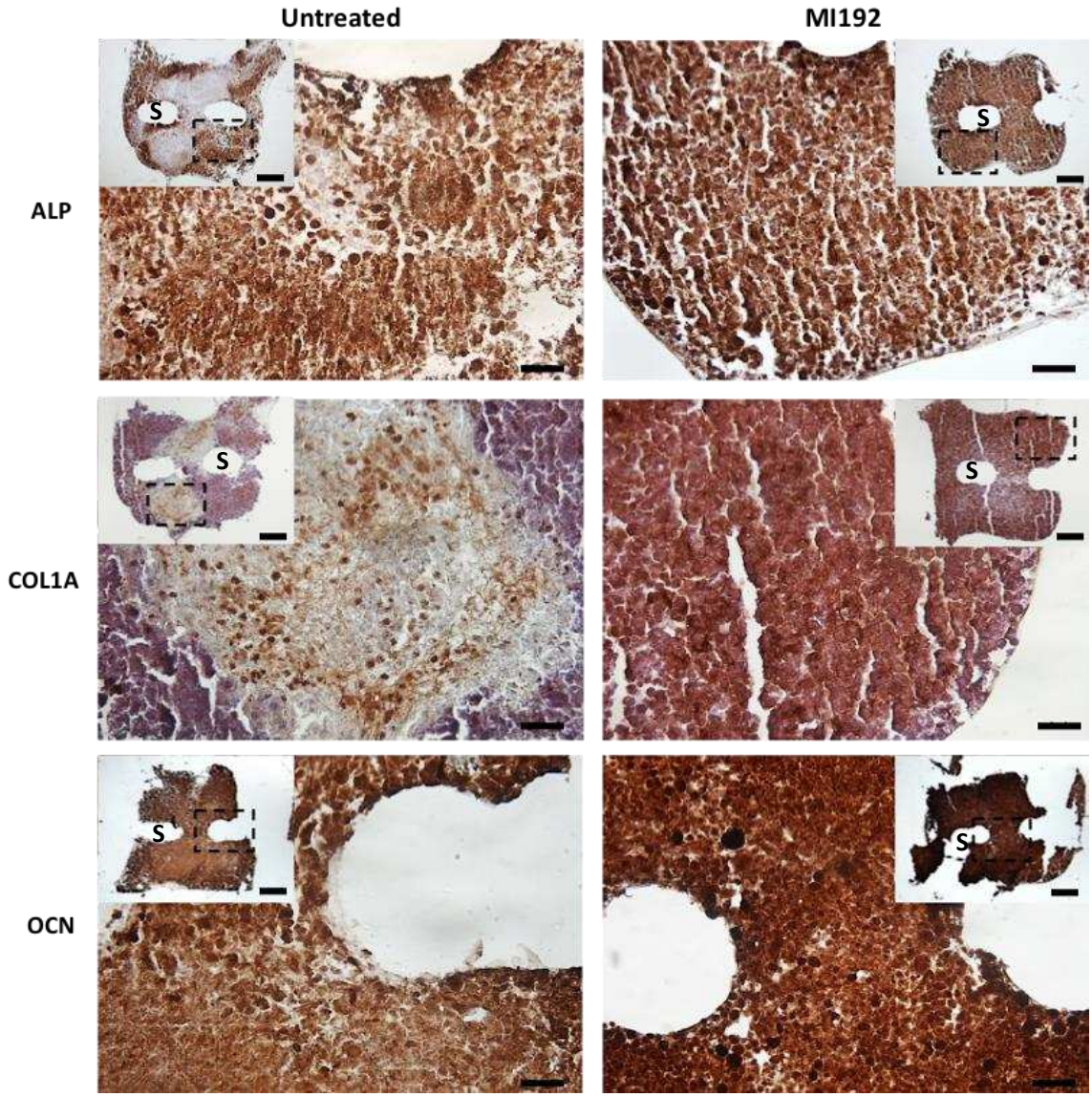

Figure 6 - Immunostaining of osteoblast-related proteins within MI192 pre-treated/untreated BMTs after 6 weeks of osteogenic culture *in vitro*. Positive immunohistochemical staining (brown), with a Harris haematoxylin counterstain (purple). Black dotted box highlight the magnified area. Scale bars = 200 and 50 μm (low and high magnification, respectively). 'S' denotes the spaces of '3D printed PEGT/PBT scaffolds', which were removed during histological processing.

MI192 enhanced hBMSCs bone-like tissue formation in 3D BMT *in vivo*

Following the assembly of untreated/MI192 pre-treated BMTs, the constructs were sealed within diffusion chambers, and these chambers containing BMT constructs were implanted intraperitoneally

within CD1 nude mice for 8 weeks. Histological analysis revealed the MI192 pre-treated BMTs exhibited increased intensity and uniform deposition of collagen when compared to the control, identified by picrosirius red analysis (Fig 7A). Moreover, the untreated constructs displayed enhanced accumulation of GAGs, where the distribution of collagens and GAGs were observed aberrantly within the BMT. Following Von Kossa staining, mineral nodules were observed throughout both BMT groups, primarily towards the outer regions of individual microtissues (Fig 7B). Mineral nodule formation was more isolated in the untreated BMT, located towards one face of the constructs. However, the MI192 BMT exhibited substantially increased mineral depositions, distributed more homogenously through the construct. The semi-quantitative analysis confirmed a significantly greater mineral nodule coverage within the MI192 pre-treated BMT (2.39-fold) compared to the untreated control (Fig 7C) ($P \leq 0.001$).

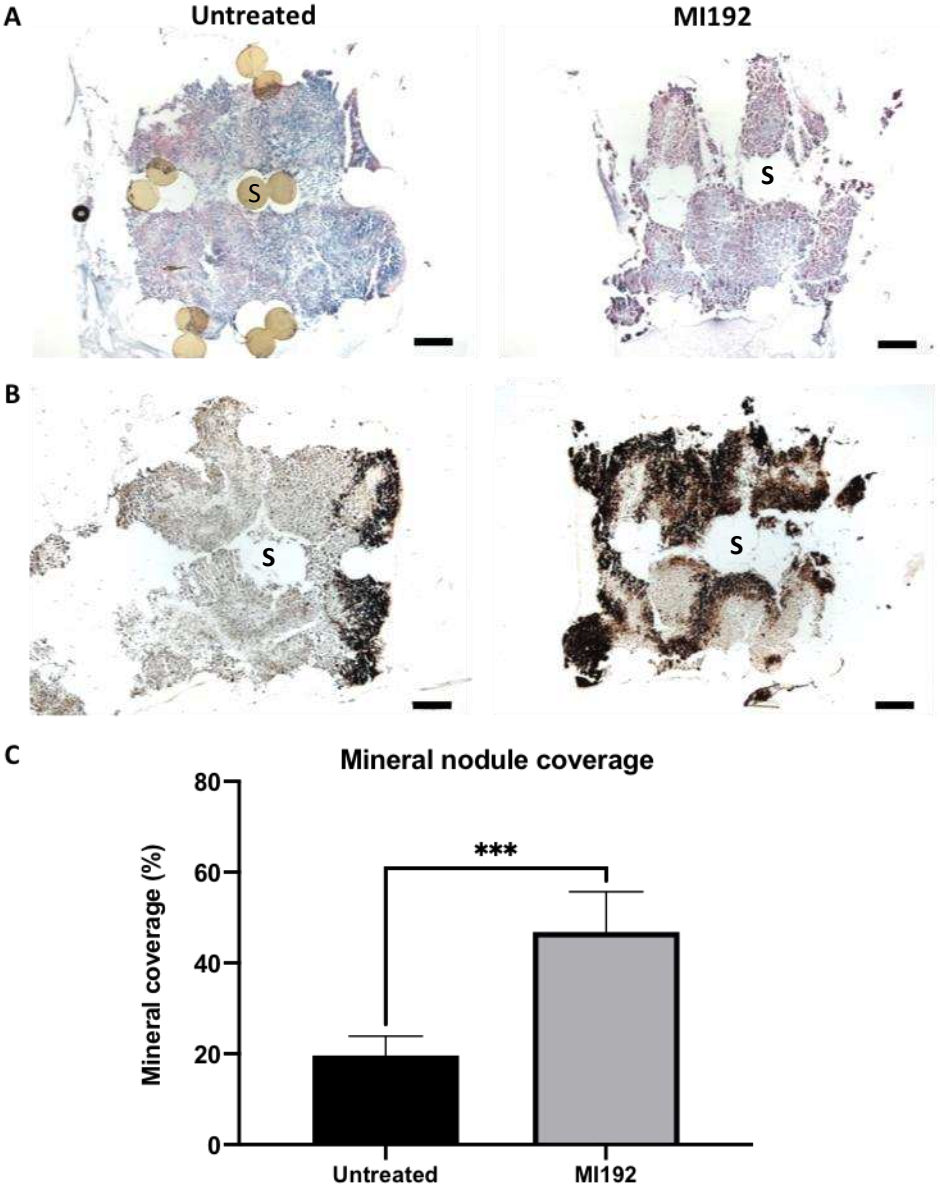

Figure 7 - Histological analysis of MI192 pre-treated hBMSC BMT constructs after *in vivo* implantation. A) Picrosirius red/Alcian blue staining for collagen/GAG depositions. (B) Von Kossa staining for mineral nodule formation. C) Percentage mineral nodule coverage on BMT samples. Scale bars = 200 μm. Data are represented

as mean ± SD (n=3). ***P ≤ 0.001. 'S' denotes the '3D printed PEGT/PBT scaffolds' (brown colour), the white spaces were due to the scaffolds removed during histological processing.

Immunohistochemical analysis showed that both untreated and MI192 treated BMT constructs exhibited positive staining for the Col1a and OCN (Fig 8). There was substantially increased Col1a expression within the MI192 BMT when compared to the untreated control. Both untreated and MI192 BMT constructs exhibited strong OCN expression. However, protein deposition was more uniformly expressed within the MI192 treated construct when compared to the untreated control.

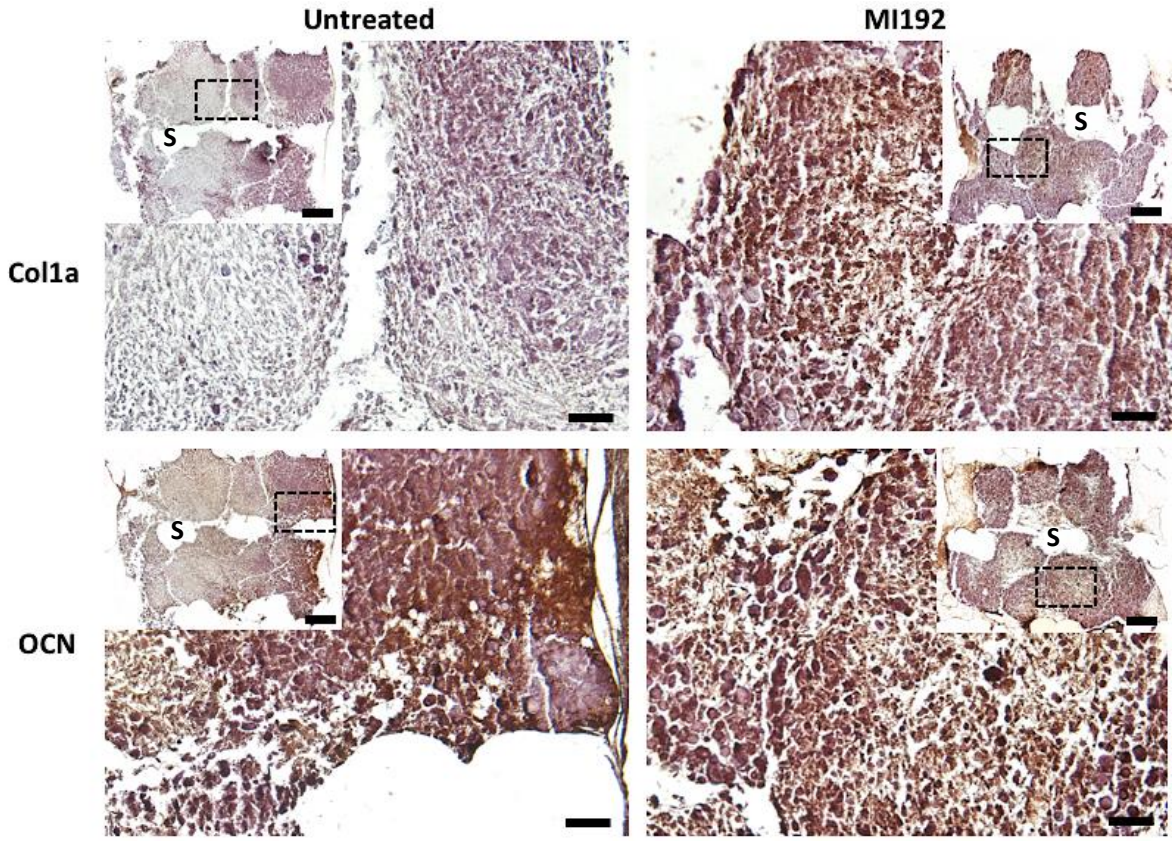

Figure 8 - Immunostaining of osteoblast-related proteins within MI192 pre-treated/untreated BMTs after *in vivo* implantation. Positive immunohistochemical staining (brown), with a Harris haematoxylin counterstain (purple). Black dotted box highlight the magnified area. Scale bars = 200 and 50 μm (low and high magnification, respectively). 'S' denotes the spaces of '3D printed PEGT/PBT scaffolds', which were removed during histological processing.

Discussion

Reprogramming the epigenome has been shown to substantially affect key cellular functions without altering the DNA sequence, therefore, possibly providing a safer alternative to controlling MSCs fate. In particular, inhibiting HDAC enzymes has shown to promote MSCs osteogenic capacity [31, 32]. Studies have demonstrated that HDAC3 is intimately linked to osteogenic differentiation [14, 15]. Hence, this study aimed to determine the effects of the HDAC2 & 3 selective inhibitor - MI192 on hBMSCs therapeutic efficacy for bone augmentation.

As MSCs are highly receptive to epigenetic changes [33, 34], the use of HDACis may provide a valuable tool for controlling MSCs functionality for bone tissue engineering. Numerous studies have

demonstrated the ability of these epigenetic regulators to initiate cell death, essential to HDACis success in cancer therapeutics [35, 36]. Due to the potential side-effects of this compound, the influence of MI192 on hBMSCs viability was assessed. MI192 caused a time-dose dependant reduction in hBMSCs viability confirmed via morphological and metabolic assessment, consistent with previous studies utilising this HDACi on leukaemia and cholangiocarcinoma cell line [16, 36]. Moreover, the findings of this study showed that MI192 significantly reduced HDAC activity in a time-dose dependent manner, consistent with previous studies with HeLa and PC3 [16, 37]. Importantly, the HDAC inhibition observed had a downstream effect on histone acetylation [31]. Therefore, MI192 treatment of ≥ 20 µM for 48 hours likely resulted in a transcriptionally permissive chromatin structure, enhancing the cell's differentiation capacity. In this study, a pre-treatment strategy was adopted due to the effects of prolonged MI192 exposure on causing a time-dose dependent reduction in hBMSCs viability, with this approach commonly implemented in the literature with the use of panHDACis such as TSA [38]. To initially determine the effects of MI192 on hBMSCs osteogenic differentiation, ALPSA, an early marker of osteogenesis, was quantified. Our findings showed that 50 µM MI192 for 48 hours prior to osteogenic culture significantly enhanced hBMSCs ALPSA compared to the untreated control. Interestingly, hBMSCs pre-treated with MI192 for 24 hours exhibited reduced ALPSA when compared to the untreated cells. These findings correlated with the histone acetylation results, indicating a causative link between the state of chromatin acetylation and the differentiation capacity of MI192 treated hBMSCs.

HDACis have been shown to regulate gene expression dues to their ability to modify the epigenome [10, 33, 35]. In this study, the expression of Runx2, a key osteogenic transcription factor [39], was significantly upregulated in the MI192 pre-treated cells at both the gene and protein level throughout osteogenic culture when compared to the untreated cells. These findings indicate that MI192 induced chromatin hyperacetylation stimulated the expression of this osteogenic transcription factor. Moreover, Jeon *et al.* (2006) demonstrated that Runx2 acetylation enhances its transcriptional activity and stability via protection from Smurf-1 mediated degradation [40]. Therefore, MI192 treatment probably increased Runx2 expression and transcriptional activity, likely attributed to modifications to the chromatin structure, protection from Smurf-1 mediated degradation and relieving HDAC3 repression. However, this would require further investigation. Our data also showed that ALP mRNA and protein expression levels were significantly upregulated in the MI192 pre-treated cells compared to the untreated control, consistent with the enhancements observed in the functional ALPSA analysis.

It is well known that both Col1a and OCN are late osteoblast-related markers. MI192 pre-treatment significantly upregulated the mRNA and protein expression levels of both markers compared to that of the untreated group. Paino *et al.* (2014) knocked out HDAC2 in dental pulp stromal cells and found that the lack of HDAC2 resulted in the downregulation of OCN gene expression [33]. Our data showed that MI192 had a positive effect on OCN expression, likely due to the MI192 specificity to HDAC3. This suggests the importance of HDAC3 in regulating hBMSCs osteogenic maturation. Studies have demonstrated that HDACis have the capacity to enhance the expression of osteoblast-related markers [32, 33], although, with the use of panHDACis, it is probable their mechanism of action relies heavily on histone modifications rather than the additional modifications to Runx2 transcriptional activity due to MI192 selective inhibition of HDAC3. Importantly, it was confirmed that MI192 promoted hBMSCs extracellular matrix mineralisation, correlating with enhanced mineralisation induced by panHDACis in the literature [12, 33]. Importantly, this was consistent with the previously reported effects of

MI192 on enhancing hDPSCs mineralisation capacity [19], indicating the plasticity of this HDACi in stimulating MSCs from different origins.

Based on these findings, the effects of MI192 on hBMSCs bone-like tissue formation was further evaluated within the BMT model due to the advantages microtissue culture provides for osteogenesis. Several studies have reported the enhanced osteogenic induction of cells cultured as microtissues when compared to conventional 2D culture. For example, Yamaguchi *et al*. (2013) reported enhanced *in vitro* mineralisation and *in vivo* bone formation capacity of rat MSCs when cultured as spheroids compared to 2D cultured cells [22]. Similarly, Baraniak *et al*. (2012) described a 5-fold increase in murine BMSCs mineralisation when compared to cells culture in 2D culture [23]. Moreover, as cells exhibit altered receptiveness to bioactive signals when cultured in 3D, it is important to investigate the influence of epigenetic reprogramming induced by MI192 on hBMSCs osteogenesis within the BMT. Our findings showed that MI192 significantly increased hBMSCs osteoblast-related gene expression during microtissue culture, consistent with the 2D culture observations. Moreover, ALPSA within the MI192 pre-treated BMT was significantly enhanced (2.41-fold) when compared to that of the untreated construct. This enhancement in ALPSA was 1.43-fold higher compared to that observed in the 2D studies, indicating the BMT microenvironment potentiates MI192 efficacy in stimulating hBMSCs osteogenesis when compared to 2D monolayer culture.

Histological analysis showed that the incorporated microtissues fused *in situ* with neighbouring microtissues, consistent with previous studies [27]. The MI192 pre-treated BMTs exhibited substantially increased expression of osteoblast-related proteins distributed more homogenously throughout the construct when compared to the aberrant protein expression observed in the untreated BMTs. This differential pattern of protein expression may indicate the role of MI192 pre-treatment in priming all cells for osteogenic differentiation in this model when compared to the untreated hBMSCs. The most intense protein deposition within the constructs was located at the periphery and at the microtissue/scaffold interface, likely attributed to increased proximity to osteogenic medium and the influence of scaffold stiffness on MSCs osteogenesis [41-43]. It is important to assess the mineralisation within the newly formed extracellular matrix, a key attribute for engineering functional bone-like tissue. Both untreated and MI192 treated hBMSCs exhibited extensive mineral deposition within the constructs, likely attributed to the favourable microtissue environment in facilitating mineralisation, such as the increased cell-cell/cell-matrix interactions inducing key cellular differentiation pathways [44-46]. In addition to promoting cellular differentiation, several studies have reported the influence of spheroid culture on the production of soluble paracrine factors such as extracellular vesicles (EVs) [47, 48], which have been reported to influence extracellular matrix mineralisation [49]. Moreover, it has been reported that EVs derived from epigenetically-modified osteoblasts significantly promoted the mineralisation of hBMSCs [50], indicating the potential role of MI192 treated hBMSCs secretome on stimulating extracellular matrix mineralisation, although this would require further investigation. In this present study, we observed a more homogenous mineral deposition throughout the MI192 BMT construct when compared to the atypical deposition observed in the untreated group, consistent with the extracellular matrix protein expression observed in this study. This provides further evidence regarding the capability of MI192 pre-treatment in "priming" all hBMSCs with increased osteogenic capacity resulting in enhanced/homogenous bone-like tissue formation within the BMT. The influence of panHDACis on MSCs osteogenesis in pellet culture has been previously investigated. For example, El-Serafi *et al*.

(2011) reported that TSA pre-treatment did not increase the mineralisation capacity of hBMSCs when cultured as cell pellets [51], which did not replicate the findings of this study. This further emphasises the importance of using selective HDACis which exhibits increased potency by targeting osteogenic-related HDAC isoforms.

There have been limited investigations in the literature examining the use of HDACis in promoting MSCs bone formation *in vivo*, with the majority of these studies utilising panHDACis. For example, Jung *et al.* (2010) reported increased osteoblast differentiation when α-calcium scaffolds loaded with the HDACis Trichostatin A (TSA) and NaB were implanted within a critical-sized rat bone defect model [52]. Similarly, Lee *et al.* (2011) demonstrated pre-soaking collagen scaffolds with the HDACi Largazole enhanced the regeneration of calvarial bone defect [53]. However, studies have reported the detrimental effect of HDACis on bone formation *in vivo*. McGee-Lawrence and Westendorf (2011) reported SAHA had a negative effect on the trabecular skeleton in C57BL/6 mice, with a reduction in osteoblast numbers [54]. Consequently, there is growing precedence to investigate the efficacy of selective HDACi compounds to stimulate bone formation *in vivo*.

In the present study, MI192 pre-treated BMTs were implanted within the intraperitoneal cavity of mice to determine their ability to promote bone formation within a more physiological environment. The use of diffusion chambers provides a 'closed' environment within the host animal to allow free exchange of nutrients/waste for the implanted HDACi-induced hBMSCs for bone formation within the BMT constructs without the direct interaction with host cells. The advantage of this model is to ensure any tissue formed within the diffusion chamber must originate from the implanted cells [55], which overcome the limitation of subcutaneous or renal capsule implantation models. Several studies have reported the use of diffusion chamber model for the assessment of bone formation *in vivo* [56-58]. It was observed that MI192 pre-treatment controlled the lineage-specific differentiation of hBMSCs, where the untreated constructs exhibited aberrant deposition of osteogenic and chondrogenic proteins, which is in support of our *in vitro* findings. Moreover, the MI192 treated groups showed substantially enhanced osteoblast-related protein expression and mineralisation within the construct, correlating with the *in vitro* analysis and several studies in the literature with panHDACis [8, 52, 53]. Interestingly, a greater fold increase in mineralisation between the MI192 treated and untreated BMT constructs were observed *in vivo* compared to *in vitro* (2.39 vs 1.67-fold). This possibly indicates the dependency of untreated hBMSCs within the BMT on the osteoinductive conditions *in vitro* to promote mineralisation, while MI192 enhanced the osteogenic capacity of hBMSCs, increasing its efficacy for bone formation *in vitro* and *in vivo*. Taken together, these *in vivo* findings provide increased pre-clinical evidence into the potential utility of epigenetic reprogramming of hBMSCs for bone formation. It would be of interest to investigate the influence of MI192 on promoting bone regeneration within a critical-sized load-bearing defect, as this would provide greater evidence into the effectiveness of this approach in a clinical setting.

Conclusion

In conclusion, these findings demonstrate that the HDAC2 & 3 selective inhibitor - MI192 is capable of reprogramming the epigenetic functionality of hBMSCs, enhancing its osteogenic capacity *in vitro* and *in vivo,* which indicates the potential of using epigenetic regulation as an engineering approach to improve MSCs therapeutic efficacy for bone augmentation strategies.

Acknowledgements

KM and XY were partially funded by the 'EPSRC Centre for Doctoral Training in Tissue Engineering and Regenerative Medicine' - Innovation in Medical and Biological Engineering, multidisciplinary collaboration of Faculties at the University of Leeds. Grant number EP/L014823/1. KM, KL, TW, and XY were partially funded by the European Union Seventh Framework Programme ([FP7/2007–2013] [FP7/2007–2011]) for 'SkelGEN' consortium under grant agreement n^{o} [318553], and XY was partially supported by the UK-China Science Bridge Award and Changzhou Science and Technology Bureau.

CRediT author statement

KM: Conceptualisation, methodology, formal analysis, investigation, data curation, writing – original draft. NM: resources. KL: resources, writing – review & editing. LJ: conceptualisation, supervision, writing – review & editing. TW: resources, writing – review & editing. XY: conceptualisation, supervision, project administration, methodology, data curation, writing – review & editing and final proof.

Ethical consideration

All animal studies were conducted under procedures approved by the University of Leeds Ethics Committee and under the UK Home Office project license (PPL: 70/8549).

Declaration of interest: None.

References

[1] Dimitriou R, Jones E, McGonagle D, Giannoudis PV. Bone regeneration: current concepts and future directions. Bmc Medicine l2011;9.

[2] Calori GM, Mazza E, Colombo M, Ripamonti C. The use of bone-graft substitutes in large bone defects: Any specific needs? Injury-International Journal of the Care of the Injured l2011;42: S56-S63.

[3] Djouad F, Guerit D, Marie M, Toupet K, Jorgensen C, Noel D. Mesenchymal Stem Cells: New Insights into Bone Regenerative Applications. Journal of Biomaterials and Tissue Engineering l2012;2: 14-28.

[4] Amini AR, Laurencin CT, Nukavarapu SP. Bone tissue engineering: recent advances and challenges. Crit Rev Biomed Eng l2012;40: 363-408.

[5] Izadpanah R, Trygg C, Patel B, Kriedt C, Dufour J, Gimble JM, Bunnell BA. Biologic properties of mesenchymal stem cells derived from bone marrow and adipose tissue. Journal of Cellular Biochemistry l2006;99: 1285-1297.

[6] Moschidou D, Mukherjee S, Blundell MP, Drews K, Jones GN, Abdulrazzak H, Nowakowska B, Phoolchund A, Lay K, Ramasamy TS, Cananzi M, Nettersheim D, Sullivan M, Frost J, Moore G, Vermeesch JR, Fisk NM, Thrasher AJ, Atala A, Adjaye J, Schorle H, De Coppi P, Guillot PV. Valproic Acid Confers Functional Pluripotency to Human Amniotic Fluid Stem Cells in a Transgene-free Approach. Molecular Therapy l2012;20: 1953-1967.

[7] Tollervey JR, Lunyak VV. Epigenetics Judge, jury and executioner of stem cell fate. Epigenetics l2012;7: 823-840.

[8] Huynh NCN, Everts V, Nifuji A, Pavasant P, Ampornaramveth RS. Histone deacetylase inhibition enhances in-vivo bone regeneration induced by human periodontal ligament cells. Bone l2017;95: 76-84.
[9] Duncan HF, Smith AJ, Fleming GJP, Cooper PR. HDACi: Cellular Effects, Opportunities for Restorative Dentistry. Journal of Dental Research l2011;90: 1377-1388.
[10] Cho HH, Park HT, Kim YJ, Bae YC, Suh KT, Jung JS. Induction of osteogenic differentiation of human mesenchymal stem cells by histone deacetylase inhibitors. Journal of Cellular Biochemistry l2005;96: 533-542.
[11] Xu Y, Hammerick KE, James AW, Carre AL, Leucht P, Giaccia AJ, Longaker MT. Inhibition of Histone Deacetylase Activity in Reduced Oxygen Environment Enhances the Osteogenesis of Mouse Adipose-Derived Stromal Cells. Tissue Engineering Part A l2009;15: 3697-3707.
[12] Xu S, De Veirman K, Evans H, Santini GC, Vande Broek I, Leleu X, De Becker A, Van Camp B, Croucher P, Vanderkerken K, Van Riet I. Effect of the HDAC inhibitor vorinostat on the osteogenic differentiation of mesenchymal stem cells in vitro and bone formation in vivo. Acta Pharmacol Sin l2013;34: 699-709.
[13] Yang SS, Zhang R, Wang G, Zhang YF. The development prospection of HDAC inhibitors as a potential therapeutic direction in Alzheimer's disease. Translational Neurodegeneration l2017;6.
[14] Schroeder TM, Kahler RA, Li XD, Westendorf JJ. Histone deacetylase 3 interacts with Runx2 to repress the osteocalcin promoter and regulate osteoblast differentiation. Journal of Biological Chemistry l2004;279: 41998-42007.
[15] Lamour V, Detry C, Sanchez C, Henrotin Y, Castronovo V, Bellahcene A. Runx2-and histone deacetylase 3-mediated repression is relieved in differentiating human osteoblast cells to allow high bone sialoprotein expression. Journal of Biological Chemistry l2007;282: 36240-36249.
[16] Boissinot M, Inman M, Hempshall A, James SR, Gill JH, Selby P, Bowen DT, Grigg R, Cockerill PN. Induction of differentiation and apoptosis in leukaemic cell lines by the novel benzamide family histone deacetylase 2 and 3 inhibitor MI-192. Leukemia Research l2012;36: 1304-1310.
[17] Demyanenko SV, Nikul VV, Uzdensky AB. The Neuroprotective Effect of the HDAC2/3 Inhibitor MI192 on the Penumbra After Photothrombotic Stroke in the Mouse Brain. Molecular Neurobiology l2020;57: 239-248.
[18] Gillespie J, Savic S, Wong C, Hempshall A, Inman M, Emery P, Grigg R, McDermott MF. Histone deacetylases are dysregulated in rheumatoid arthritis and a novel histone deacetylase 3-selective inhibitor reduces interleukin-6 production by peripheral blood mononuclear cells from rheumatoid arthritis patients. Arthritis and Rheumatism l2012;64: 418-422.
[19] Man KL, L.; Jiang, L.-H.; Yang, X.B. The Selective Histone Deacetylase Inhibitor MI192 Enhances the Osteogenic Differentiation Efficacy of Human Dental Pulp Stromal Cells. International Journal of Molecular Sciences l2021;22: 1-17.
[20] Baker BM, Chen CS. Deconstructing the third dimension - how 3D culture microenvironments alter cellular cues. Journal of Cell Science l2012;125: 3015-3024.
[21] Abbott A. Cell culture: Biology's new dimension. Nature l2003;424: 870-872.
[22] Yamaguchi Y, Ohno J, Sato A, Kido H, Fukushima T. Mesenchymal stem cell spheroids exhibit enhanced in-vitro and in-vivo osteoregenerative potential. Bmc Biotechnology l2014;14.

596 [23] Baraniak PR, McDevitt TC. Scaffold-free culture of mesenchymal stem cell spheroids
597 in suspension preserves multilineage potential. Cell and Tissue Research l2012;347: 701-711.
598 [24] Langenbach F, Naujoks C, Smeets R, Berr K, Depprich R, Kubler N, Handschel J.
599 Scaffold-free microtissues: differences from monolayer cultures and their potential in bone
600 tissue engineering. Clinical Oral Investigations l2013;17: 9-17.
601 [25] Wang W, Itaka K, Ohba S, Nishiyama N, Chung UI, Yamasaki Y, Kataoka K. 3D spheroid
602 culture system on micropatterned substrates for improved differentiation efficiency of
603 multipotent mesenchymal stem cells. Biomaterials l2009;30: 2705-15.
604 [26] Schon BS, Hooper GJ, Woodfield TB. Modular Tissue Assembly Strategies for
605 Biofabrication of Engineered Cartilage. Ann Biomed Eng l2016.
606 [27] Schon BS, Schrobback K, van der Ven M, Stroebel S, Hooper GJ, Woodfield TBF.
607 Validation of a high-throughput microtissue fabrication process for 3D assembly of tissue
608 engineered cartilage constructs. Cell and Tissue Research l2012;347: 629-642.
609 [28] Mekhileri NV, Lim KS, Brown GCJ, Mutreja I, Schon BS, Hooper GJ, Woodfield TBF.
610 Automated 3D bioassembly of micro-tissues for biofabrication of hybrid tissue engineered
611 constructs. Biofabrication l2018;10: 024103.
612 [29] Hajighasemi F, Tajik S. Assessment of Cytotoxicity of Dimethyl Sulfoxide in Human
613 Hematopoietic Tumor Cell Lines
614 Iranian Journal of Blood & Cancer l2017;9: 48-53.
615 [30] de Abreu Costa L, Henrique Fernandes Ottoni M, Dos Santos MG, Meireles AB, Gomes
616 de Almeida V, de Fatima Pereira W, Alves de Avelar-Freitas B, Eustaquio Alvim Brito-Melo G.
617 Dimethyl Sulfoxide (DMSO) Decreases Cell Proliferation and TNF-alpha, IFN-gamma, and IL-2
618 Cytokines Production in Cultures of Peripheral Blood Lymphocytes. Molecules l2017;22.
619 [31] Hu XQ, Fu YT, Zhang X, Dai LH, Zhu JX, Bi ZG, Ao YF, Zhou CY. Histone deacetylase
620 inhibitor sodium butyrate promotes the osteogenic differentiation of rat adipose- derived
621 stem cells. Development Growth & Differentiation l2014;56: 206-213.
622 [32] Huynh NC, Everts V, Pavasant P, Ampornaramveth RS. Inhibition of Histone
623 Deacetylases Enhances the Osteogenic Differentiation of Human Periodontal Ligament Cells.
624 J Cell Biochem l2016;117: 1384-95.
625 [33] Paino F, La Noce M, Tirino V, Naddeo P, Desiderio V, Pirozzi G, De Rosa A, Laino L,
626 Altucci L, Papaccio G. Histone Deacetylase Inhibition with Valproic Acid Downregulates
627 Osteocalcin Gene Expression in Human Dental Pulp Stem Cells and Osteoblasts: Evidence for
628 HDAC2 Involvement. Stem Cells l2014;32: 279-289.
629 [34] Sharma S, Bhonde R. Genetic and epigenetic stability of stem cells: Epigenetic
630 modifiers modulate the fate of mesenchymal stem cells. Genomics l2020;112: 3615-3623.
631 [35] Schroeder TM, Nair AK, Staggs R, Lamblin AF, Westendorf JJ. Gene profile analysis of
632 osteoblast genes differentially regulated by histone deacetylase inhibitors. Bmc Genomics
633 l2007;8.
634 [36] Yin YY, Zhang MM, Dorfman RG, Li Y, Zhao ZG, Pan YD, Zhou Q, Huang S, Zhao SM, Yao
635 YL, Zou XP. Histone deacetylase 3 overexpression in human cholangiocarcinoma and
636 promotion of cell growth via apoptosis inhibition. Cell Death & Disease l2017;8.
637 [37] Bacon T, Seiler C, Wolny M, Hughes R, Watson P, Schwabe J, Grigg R, Peckham M.
638 Histone deacetylase 3 indirectly modulates tubulin acetylation. Biochemical Journal
639 l2015;472: 367-377.
640 [38] Maroni P, Brini AT, Arrigoni E, de Girolamo L, Niada S, Matteucci E, Bendinelli P,
641 Desiderio MA. Chemical and genetic blockade of HDACs enhances osteogenic differentiation

of human adipose tissue-derived stem cells by oppositely affecting osteogenic and adipogenic transcription factors. Biochem Biophys Res Commun l2012;428: 271-7.
[39] Jonason JH, Xiao G, Zhang M, Xing L, Chen D. Post-translational Regulation of Runx2 in Bone and Cartilage. Journal of Dental Research l2009;88: 693-703.
[40] Jeon EJ, Lee KY, Choi NS, Lee MH, Kim HN, Jin YH, Ryoo HM, Choi JY, Yoshida M, Nishino N, Oh BC, Lee KS, Lee YH, Bae SC. Bone morphogenetic protein-2 stimulates Runx2 acetylation. Journal of Biological Chemistry l2006;281: 16502-16511.
[41] Ghasemi-Mobarakeh L, Prabhakaran MP, Tian LL, Shamirzaei-Jeshvaghani E, Dehghani L, Ramakrishna S. Structural properties of scaffolds: Crucial parameters towards stem cells differentiation. World Journal of Stem Cells l2015;7: 728-744.
[42] Shih YRV, Tseng KF, Lai HY, Lin CH, Lee OK. Matrix Stiffness Regulation of Integrin-Mediated Mechanotransduction During Osteogenic Differentiation of Human Mesenchymal Stem Cells. Journal of Bone and Mineral Research l2011;26: 730-738.
[43] Engler AJ, Sen S, Sweeney HL, Discher DE. Matrix elasticity directs stem cell lineage specification. Cell l2006;126: 677-689.
[44] Langenbach F, Naujoks C, Laser A, Kelz M, Kersten-Thiele P, Berr K, Depprich R, Kubler N, Kogler G, Handschel J. Improvement of the Cell-loading Efficiency of Biomaterials by Inoculation with Stem Cell-based Microspheres, in Osteogenesis. Journal of Biomaterials Applications l2012;26: 549-564.
[45] Langenbach F, Berr K, Naujoks C, Hassel A, Hentschel M, Depprich R, Kubler NR, Meyer U, Wiesmann HP, Kogler G, Handschel J. Generation and differentiation of microtissues from multipotent precursor cells for use in tissue engineering. Nature Protocols l2011;6: 1726-1735.
[46] Hildebrandt C, Buth H, Thielecke H. A scaffold-free in vitro model for osteogenesis of human mesenchymal stem cells. Tissue & Cell l2011;43: 91-100.
[47] Man K, Brunet MY, Jones MC, Cox SC. Engineered Extracellular Vesicles: Tailored-Made Nanomaterials for Medical Applications. Nanomaterials l2020;10.
[48] Cha JM, Shin EK, Sung JH, Moon GJ, Kim EH, Cho YH, Park HD, Bae H, Kim J, Bang OY. Efficient scalable production of therapeutic microvesicles derived from human mesenchymal stem cells. Scientific Reports l2018;8.
[49] Cui L, Houston DA, Farquharson C, MacRae VE. Characterisation of matrix vesicles in skeletal and soft tissue mineralisation. Bone l2016;87: 147-158.
[50] Man K, Brunet, M. Y., Fernandez-Rhodes, M., Williams, S., Heaney, L. M., Gethings, L. A., Federici, A., Davies, O. G., Hoey, D., & Cox, S. C. Epigenetic reprogramming enhances the therapeutic efficacy of osteoblast-derived extracellular vesicles to promote human bone marrow stem cell osteogenic differentiation. Journal of Extracellular Vesicles l2021;10.
[51] El-Serafi AT, Oreffo RO, Roach HI. Epigenetic modifiers influence lineage commitment of human bone marrow stromal cells: Differential effects of 5-aza-deoxycytidine and trichostatin A. Differentiation l2011;81: 35-41.
[52] Jung HM, Song GA, Lee YK, Baek JH, Ryoo HM, Kim GS, Choung PH, Woo KM. Modulation of the resorption and osteoconductivity of alpha-calcium sulfate by histone deacetylase inhibitors. Biomaterials l2010;31: 29-37.
[53] Lee SU, Kwak HB, Pi SH, You HK, Byeon SR, Ying Y, Luesch H, Hong J, Kim SH. In Vitro and In Vivo Osteogenic Activity of Largazole. ACS Med Chem Lett l2011;2: 248-251.
[54] McGee-Lawrence ME, McCleary-Wheeler AL, Secreto FJ, Razidlo DF, Zhang MZ, Stensgard BA, Li XD, Stein GS, Lian JB, Westendorf JJ. Suberoylanilide hydroxamic acid (SAHA; vorinostat) causes bone loss by inhibiting immature osteoblasts. Bone l2011;48: 1117-1126.

[55] Jones E, **Yang XB**, McGonagle D, Giannoudis P. Animal Models for Investigating MSC Involvement in Bone and Cartilage Repair. In: Jones E, **Yang XB**, McGonagle D, Giannoudis P, editors. Skeletal Regeneration and Mesenchymal Stem cells. Oxford: Elsevier; 2013.
[56] Yang XBB, Whitaker MJ, Sebald W, Clarke N, Howdle SM, Shakesheff KM, Oreffo ROC. Human osteoprogenitor bone formation using encapsulated bone morphogenetic protein 2 in porous polymer scaffolds. Tissue Engineering l2004;10: 1037-1045.
[57] Yang XB, Tare RS, Partridge KA, Roach HI, Clarke NM, Howdle SM, Shakesheff KM, Oreffo RO. Induction of human osteoprogenitor chemotaxis, proliferation, differentiation, and bone formation by osteoblast stimulating factor-1/pleiotrophin: Osteoconductive biomimetic scaffolds for tissue engineering. Journal of Bone and Mineral Research l2003;18: 47-57.
[58] Gundle R, Joyner CJ, Triffitt JT. Human Bone Tissue Formation in-Diffusion Chamber Culture in-Vivo by Bone-Derived Cells and Marrow Stromal Fibroblastic Cells. Bone l1995;16: 597-601.

738
739
740
741 **Supplementary figures**
742
743
744 **Supplementary Table 1 - Primers used for TaqMan gene expression assays**

Gene symbol	Description	TaqMan identification
GAPDH	Glyceraldehyde-3-phosphate dehydrogenase	Hs99999905_m1
RUNX2	Runt-related transcription factor 2	Hs00231692_m1
ALPL	Alkaline phosphatase	Hs01029144_m1
COL1A1	Collagen, type I	Hs00164004_m1
OCN/BGLAP	Osteocalcin/PMF-bone gamma- carboxyglutamate (gla) protein	Hs00609452_g1

745
746
747
748
749 **Supplementary Table 2 - Primary antibodies used for ICW and immunohistochemistry**

Antibody	Catalogue number	Dilution
***In vitro* studies**		
Runx2	ab76956	1/600
Alkaline Phosphatase	ab126820	1/500
Collagen type I	ab6308	1/100
Osteocalcin	ab13420	1/800
***In vivo* studies**		
Collagen type I	ab138492	1/100
Osteocalcin	ab198228	1/200

750

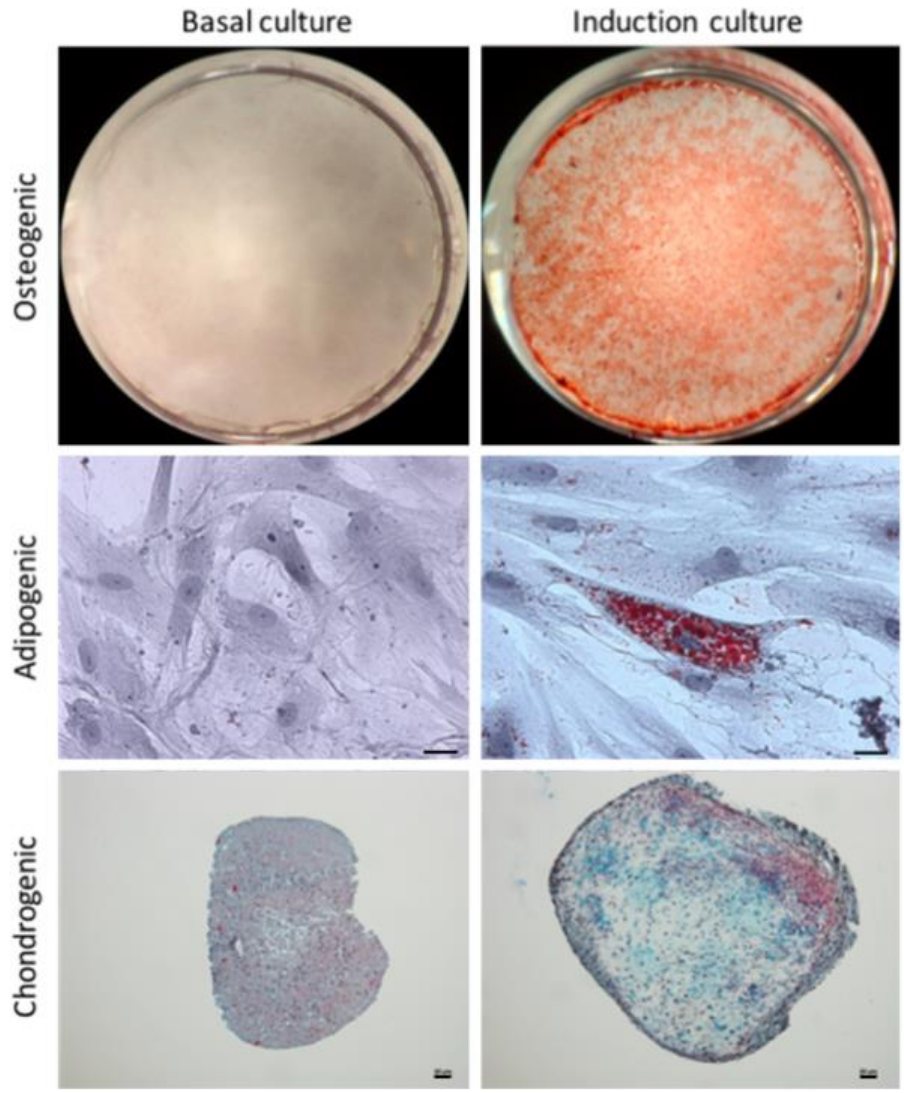

751

752 **Supplementary Figure 1 - Multi-lineage potential of hBMSCs.** Osteogenic differentiation: Positive
753 calcium accumulation was observed after 28 days cultured in osteogenic medium confirmed by
754 Alizarin Red staining; Adipogenic differentiation: lipid droplet formation was observed in hBMSCs
755 after 14 days culture in adipogenic induction medium after Oil red O staining (Scale bar = 50 µm);
756 Chondrogenic differentiation: hBMSCs were capable of forming cartilage like pellets after 21 days
757 cultured as pellets in chondrogenic induction medium, stained blue for GAGs (Alcian blue staining)
758 and red for collagen (Picrosirius red staining). Scale bar = 20 µm.

759